Kodaikanal Obs. Bull. Ser. A (1977) 2, 34—41

INTENSITY FLUCTUATIONS IN THE SOLAR CHROMOSPHERE

K. R. SIVARAMAN and P. P. VENKITACHALAM

ABSTRACT

High resolution spectrograms of the Balmer lines obtained at five positions from the centre to the limb have been used to study the r.m.s. intensity fluctuations and their dependence on the heliocentric angle. The intensity fluctuations at the line centre as well as at several wavelength positions within the lines have been derived and the variation of these fluctuations within the lines have been studied.

Key Words : Balmer lines—intensity fluctuations—solar chromosphere

1. Introduction

It has long been recognised that the temperature and density distributed throughout the chromosphere exhibit variations both in space and time. De Jager (1957) studied the total brightness fluctuations associated with the inhomogeneities of all sizes put together in the Balmer lines using spectroheliograms. Evans and Michard (1962) measured the brightness fluctuations in a number of lines representative of the photosphere and chromosphere, all at the centre of the disc and mainly in the line cores. Similar analyses have been made in different spectral lines using high resolution observations (Bappu, 1964; Canfield and Mehltretter, 1973). Cannon and Wilson (1970, 1971) studied the central intensity and velocity fluctuations in the MgI b and NaI D lines and their centre-limb variations using a radial slit. These lines essentially pertain to the low chromosphere. The use of a radial slit sets a severe limit on the number of independent samples on the solar surface that could be examined for such variations within a defined μ value. The need for understanding the spatial behaviour of the chromospheric elements by extending the study to other lines needs no emphasis.

Our aim in this analysis is to find (i) the dependence of the relative r.m.s. brightness fluctuations on the heliocentric angle and on the different wavelength positions within the line and (ii) contribution by the structures of different sizes to the observed fluctuations.

2. The Observations and Reductions

Our experimental data consists of spectra of Hα, Hβ, Hγ and Hδ obtained at the 38-cm solar tower telescope at Kodaikanal. The telescope provides an image in the slit plane with a scale of 6.5″mm^{-1}. The 18 metre Littrow spectrograph has a Babcock grating with 600 grooves mm^{-1}. The overlapping orders of the grating were eliminated with wide band Corning or Schott glass filters. Many spectra were obtained on days when the seeing was very good or excellent. From among these, those plates obtained on days with consistently good seeing, when the spatial resolution was 1 sec of arc or better were chosen for the present study. The spectra were calibrated in each case with a six-step wedge and an out of focus image of the Sun. Details of the spectra are given in Table 1.

The spectra were obtained at five positions on the disc coinciding with $\mu = 1.0$, 0.8, 0.6, 0.4 and 0.3. Density tracings for each exposure, along the core of the line as well as at different wavelength positions within each line, located at equal $\pm\Delta\lambda$ positions on either wing, were digitised at equispaced intervals corresponding to 600 km on the Sun. For the Hα and Hβ spectra obtained with a slit 50 mm long, (or 2×10^5 km on the Sun) we have density values at 332 points along the slit and for Hγ and Hδ spectra taken with a 20 mm long slit, there are 130 density values. Thus for the five μ positions together we have 4.3×10^4 density readings for Hα and Hβ and 8.5×10^3 readings for Hγ and Hδ. These density readings were then converted into relative intensities via the calibration curve with the IBM 360 computer.

Table 1. Details of the Spectra

Plate No.	Date	Line	Slit width in microns	Grating order and dispersion	Emulsion	Exposure	Scanning aperture in microns	Seeing in arc sec.
A 752 A 753 A 754	7-3-66 8-3-66	Hα	150	IV 7.15mm/Å	IV E Plate	8 sec	80x40	≈1
A 1273 A 1274	29-5-74	Hβ	100	V 7.97mm/Å	103a-0 Plate	4 sec and 5 sec	160x40	≈1.5
A 911 A 912	7-5-68	Hγ	150	VI 9.70mm/Å	103a-0 35mm film	3 sec and 5 sec	160x40	≈1
A 913 A 914	7-5-68	Hδ	150	VI 10.48mm/Å	103a-0 35mm film	3 sec and 5 sec	160x40	≈1

We now proceed to compute the power spectrum of the intensity fluctuations. The autocorrelation function Q (τ) at lag τ was computed for the intensity fluctuations for the positions $\Delta\lambda = 0.0, \pm 0.2, \pm 0.3, \pm 0.5$ and $\pm$ 0.6Å. The corresponding power spectra p(f) at frequency f were then obtained from the Fourier transform of Q (τ) by standard methods (Blackman and Tukey 1958). Figure 1 shows the power spectra of the brightness fluctuation in Hα at $\Delta\lambda = 0.0, 0.3, 0.4$ and 0.5Å. There is a hierarchy of sizes for the elements, which are brought out clearly in the power spectrum. Similar spectra for the other lines show that they can be conveniently grouped into three classes containing structures with sizes in the following ranges :

1. Class A from 1,200 to 6,000 km
2. Class B from 6,000 to 15,000 km
3. Class C from 15,000 to 35,000 km

With a sampling interval of 600 km (on the Sun) of the density readings, our Nyquist frequency corresponded to a wavelength of 1200 km. Class A represents the fine mottles, Class B covers the coarse mottles and the supergranular network boundaries are covered by Class C.

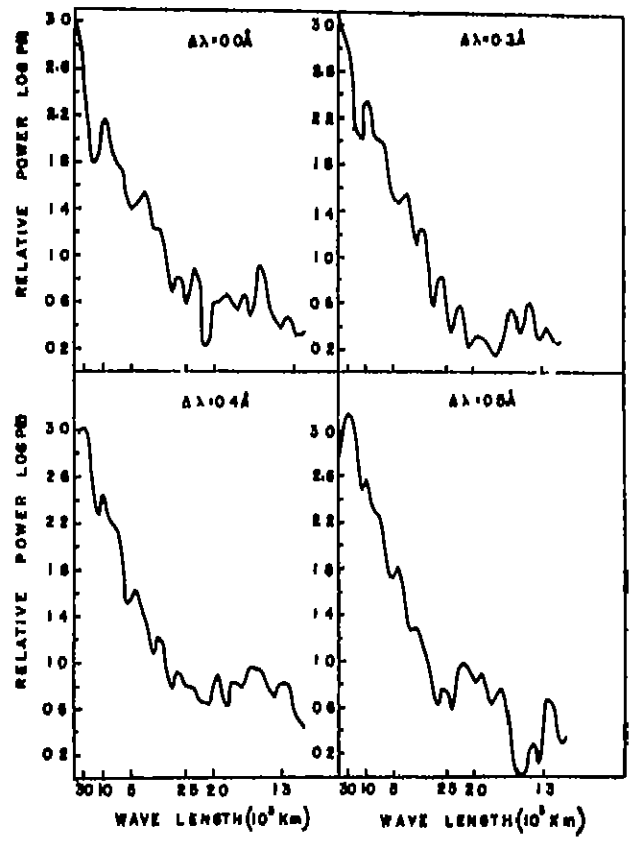

Fig. 1 Unfiltered power spectra of the brightness fluctuations for four wavelength positions within the Hα line at $\mu = 1.0$

Filtering of the raw data into three classes A, B and C was done using a zero phase shift high pass digital filter with 9 weights for Class A, 25 weights for Class B and 59 weights for Class C, following Behanon and Ness (1966). A sharp-cut-off filter has the concomitant disturbing effects due to large side lobes through which considerable leakage can occur. We have used filters with sine termination to keep the leakage through the side lobes to a minimum possible value. Filtering by such sine-terminated filters is not, however, ideal and possibly contains a minor contribution from higher wavelengths than indicated in our classification. The original data were smoothed first with the 9 weight high pass filter and then with the 25 weight filter. The 25 weight filter output was then subtracted from the corresponding values of the 9 weights filter output. This results in a series, containing intensity fluctuations contributed by only elements of Class B. Similarly, filtering was done for Class C. In the case of A, the smoothed values of the original data with the 9 point weight filter were subtracted from the corresponding values of the original series. Such filtering was done for all the wavelength positions within the Hα, Hβ, Hγ and Hδ lines and for the five μ positions for each line. The next step was to compute the r.m.s. intensity fluctuations defined by $[\Sigma(\Delta I/I)^2/N]^{1/2}$ for each class. The results give the contribution to the r.m.s. fluctuations by the elements of the A, B, C class separately, for all the wavelength positions and their variation as a function of the heliocentric angle.

These r.m.s. brightness values are not corrected for seeing and the finite width of the scanning aperture. We estimated these corrections following Canfield and Mehltretter (1973) and found that these did not increase the r.m.s. values significantly.

3. Results and Discussions

3.1 General

Figure 2 shows a plot of the intensity fluctuations along the slit in the Hα line for the various $\Delta\lambda$ s and for $\mu = 1.0$. The small-scale features are well resolved.

The line core fluctuations show very well the fine mottles — both bright and dark. These bright and dark mottles present rather a confusing pattern and the chromospheric network boundaries are barely recognisable. But as one proceeds towards the wings, they stand out clearly. This is reflected in the power spectrum which does not show a peak around 30,000km below $\Delta\lambda = 0.4$Å. From $\Delta\lambda = 0.4$Å, on-

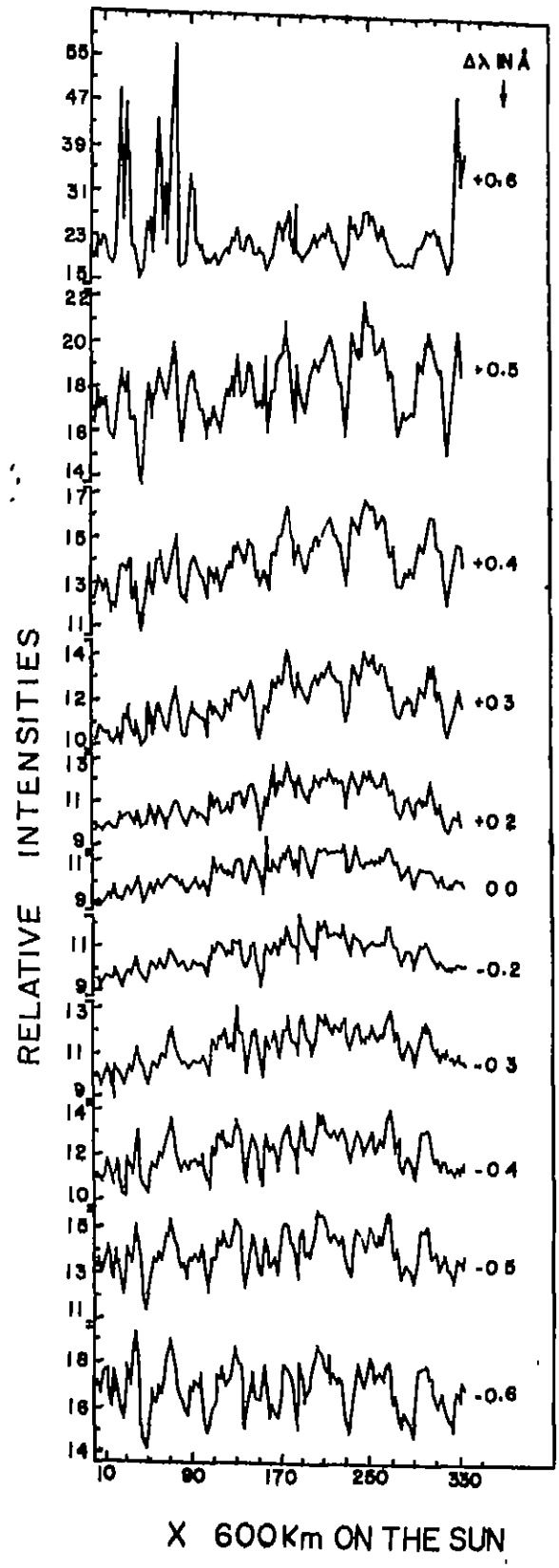

Fig. 2 Intensity fluctuations along the slit at different wavelength positions within the Hα line ($\mu = 1.0$).

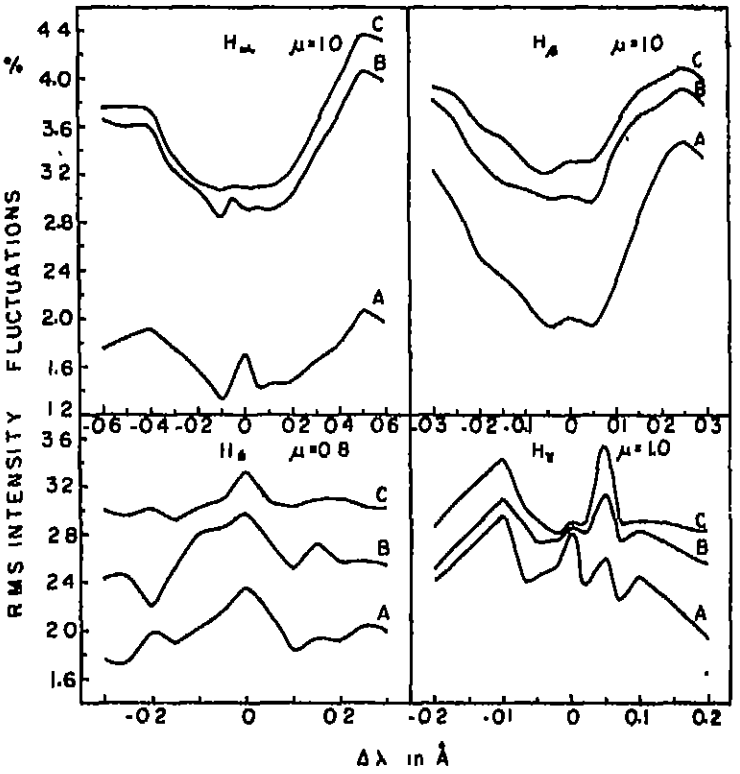

Fig 3 $\Delta\lambda$ dependence of the relative r.m.s. intensity fluctuations for $H\alpha$, $H\beta$, $H\gamma$ and $H\delta$ lines. A, B, C denote the three classes of the structure sizes.

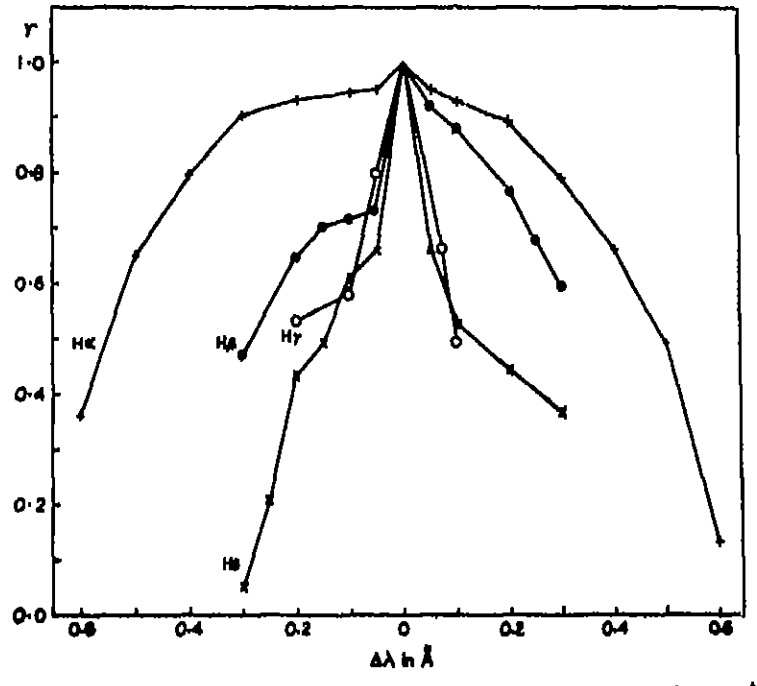

Fig 4 Coefficients of correlation r, between the line core intensity fluctuations and those at different $\Delta\lambda$ (Å) positions in the four Balmer lines ($\mu = 1.0$). The curves for other μ values are similar.

wards the peak at this wavelength is pronounced. From the intensity plot for $\Delta\lambda = +0.5$ Å one can go back to the line core plot and then identify the network boundaries. In the line core the boundaries are bright, but slowly reverse in sign and also gain in contrast as $\Delta\lambda$ increases and at $\Delta\lambda = 0.4$ Å or 0.5 Å what strikes one most is the dark network boundaries.

From a similar plot of the intensity fluctuations in the Hβ line, the chromospheric network can be identified easily from the line core fluctuations. Even at the line core, the network has only dark mottles along its boundary. Also, at no wavelength position in Hβ do we find bright mottles at the cell boundaries as seen in the Hα line core. If one goes only by this criterion one can assign the correspondence Hα 0.5Å – Hβ 0.0Å. The mottles seen in Hβ are not as contrasty as those in Hα. The Hγ and Hδ intensity plots bear close resemblance to that of Hβ. The mottles seen in Hβ, Hγ and Hδ are no longer finely resolved as in the core of Hα. Even in Hα, beyond $\Delta\lambda = 0.3$ Å, the structures overlap and appear very diffuse even under high resolution. This is obvious, as the line of sight now intercepts many elements at lower levels.

Table 2 to 5 give the r.m.s. intensity fluctuations measured in the 4 lines. The fluctuations in the Hα core at $\mu = 1.0$ for all the 3 classes put together add up to 7.7%. It is of interest to note that Evans and Michard (1962) obtained 7.8% for the r.m.s. value in the Hα core for their unfiltered data.

3.2 *Dependence on the size of the structures*

In all the lines, the amplitude of the r.m.s. brightness fluctuations increases with increasing structure size. At lower levels e.g. for NaI D and MgI b lines the r.m.s. amplitude decreases with increasing structure size, (Cannon and Wilson 1970, 1971). At these and at still lower levels, the contrast in the smaller structures is more. It may not be unreasonable to make a conjecture that here the magnetic fields are confined to finer elements and hence the heating caused in the presence of these magnetic fields are also confined to the finer elements of size 1000 km or less. This being the case, these structures which appear bright due to excess heating will form the important contributors to the overall r.m.s. intensity fluctuations, in view of the concentrated intensity at these points. At higher levels, the magnetic fields diverge sufficiently and fill in the larger and wider chromospheric network which possesses a higher intensity in virtue of a larger area of emission.

3.3 *Variation of r.m.s. fluctuations with* μ

The r.m.s. fluctuations show in general two maxima with a pronounced dip around $\mu = 0.6$ or $\mu = 0.4$. The photospheric lines Mg 4571, Na 5688 (Cannon and Wilson 1971) have a tendency to show a single maximum around $\mu = 0.8$ whereas, the stronger lines like the MgI b lines and NaI D lines show two peaks with a minimum around $\mu = 0.6$ and around $\mu = 0.8$ respectively. One is tempted to conclude that the chromospheric lines possess a double peaked structure with a dip in between, whereas the photospheric lines show a single maximum around $\mu = 0.8$ and this changeover takes place around the levels of origin of the NaI D and MgI b lines in the solar atmosphere.

3.4 *Visibility of structures*

Figure 3 shows the variation of r.m.s. intensity with $\Delta\lambda$ for each of the lines. The curves represent the visibility of the structures at these $\Delta\lambda$ positions. In Hα and Hβ the magnitude of the intensity fluctuations increases from the core outwards. In Hα the maximum visibility of the structures occurs around $\Delta\lambda = 0.5$Å and in Hβ around $\Delta\lambda = 0.3$Å. In Hγ the contrast is maximum around $\Delta\lambda = 0.05$Å, while in Hδ the intensity fluctuations decrease from the core towards the wings of the lines and the maximum visibility of the structures occurs at the line core. The asymmetry in the contrast curve is strikingly seen; the red wing being more contrasty than the violet wing. This difference is also seen in the intensity plot of Figure 2. In the case of the Balmer lines, the line is widened when it is red shifted. The correlation between the local widening and Doppler shifts causes the asymmetry (De Jager, 1957).

3.5 *Correlation of brightness at different* $\Delta\lambda$ *values*

The correlation of the intensities at the line centre with those at different $\Delta\lambda$ values decreases fast with increase in $\Delta\lambda$ but never becomes negative for the wavelength region investigated. Figure 4 shows this variation for all the 4 lines. The rapid fall in correlation in Hβ has also been noticed by Evans and Catalano (1972).

Table 2. Relative r.m.s. intensity fluctuations in per cent in Hα
A, B and C stand for the respective sizes

Δλ in Å		μ=1.0	0.8	0.6	0.4	0.3
− 0.05	A	1.5	1.3	1.4	2.1	1.4
	B	3.0	2.8	2.7	2.8	2.6
	C	3.1	3.2	3.0	3.2	3.1
− 0.10	A	1.3	1.4	1.1	1.8	1.1
	B	2.8	2.8	2.7	2.8	2.6
	C	3.1	3.2	3.1	3 3	3.1
− 0.20	A	1.5	1.8	1.2	1.7	1.3
	B	3.1	3.1	2.8	2.8	2.7
	C	3.1	3.3	3.1	3.4	3.1
− 0.30	A	1.8	2.0	1.6	1.6	1.2
	B	3.2	3.7	3.2	2.9	2.8
	C	3.3	3.6	3.4	3.5	3.2
− 0.40	A	1.9	2.2	2.0	1.7	2.6
	B	3.6	3.2	3.9	3.2	3.4
	C	3.7	3.8	3.9	3.7	3.6
− 0.50	A	1.8	2.3	1.8	2.0	1.7
	B	3.6	3.2	3.6	3.6	3.6
	C	3.8	3.7	3.6	3.7	3.7
− 0.60	A	1.8	—	—	2.3	1.9
	B	3.7	—	--	3.9	3.6
	C	3 8	—	-	3.5	3.6
0.00	A	1.7	1.4	1.2	1.6	1.2
	B	2.9	2.8	2.6	2.7	2.6
	C	3.1	3.2	3.0	3.2	3.1
+ 0.05	A	1.4	1.3	1.1	1.4	1.2
	B	2 9	2.8	2.6	2.6	2.6
	C	3.1	3.2	3.0	3.1	3.1
+ 0.10	A	1.5	1.3	1.1	1.7	1.2
	B	2.9	2.8	2.6	2.7	2.6
	C	3.1	3.2	3.0	3.1	3.1
+ 0.20	A	1.5	1.6	1.3	1.4	1.0
	B	3.0	3.1	2.7	2.6	2.6
	C	3.2	3.3	3.1	3.1	3.2
+ 0.30	A	1.7	1.7	1.4	1.4	2.2
	B	3.4	3.6	3.0	2.8	2.9
	C	3.6	3.5	3.3	3.2	3.3
+ 0.40	A	1.8	1.5	1.7	1.9	1.7
	B	3.7	3.6	3.8	3.6	3 6
	C	4.0	3.7	3.8	3.3	3.8
+ 0.50	A	2.1	2.1	1.7	2.2	1.9
	B	4.1	3.9	3.6	3.7	3.8
	C	4.3	3.5	3.5	3.4	3.8
+ 0.60	A	1.9	—	—	2.9	1 6
	B	3.4	—	—	3.5	3.5
	C	4.3	—	—	3.1	3.4

Table 3. Relative r.m.s. intensity fluctuations in per cent in Hβ
A, B and C stand for the respective sizes

Δλ in Å		μ=1.0	0.8	0.6	0.4	0.3
− 0.05	A	1.9	2.0	1.8	1.9	1.9
	B	3.0	3.0	2.9	2.8	2.9
	C	3.2	3.4	3.5	3.3	3.4
− 0.10	A	2.2	2.0	1.8	1.9	1.9
	B	3.1	3.5	3.0	2.7	2.9
	C	3.3	4.0	3.8	3.3	3.4
− 0.15	A	2.4	2.2	1.9	2.2	2.7
	B	3.1	4.1	3.0	2.9	3.5
	C	3.5	4.3	3.7	3.4	4.4
− 0.20	A	2.5	2.6	2.1	2.3	2.4
	B	3.3	4.2	3.1	3.1	3.5
	C	3.6	4.6	3.6	3.8	4.4
− 0.25	A	3.0	2.9	2.3	2.4	2.6
	B	3.7	4.3	3.2	3.3	3.8
	C	3.9	4.5	4.0	3.9	4.5
− 0.30	A	3.2	2.8	2.4	2.9	3.8
	B	3.8	4.2	3.1	3.8	4.1
	C	3.9	4.4	3.8	4.3	4.8
0.00	A	2.0	2.1	2.2	1.8	2.0
	B	3.1	3.0	2.9	2.7	2.8
	C	3.3	3.3	3.6	3.3	3.4
+ 0.05	A	1.9	2.1	1.9	1.9	1.8
	B	3.0	3.1	2.9	2.8	2.9
	C	3.3	3.4	3.4	3.3	3.4
+ 0.10	A	2.3	2.5	2.0	2.2	1.9
	B	3.4	3.0	2.9	2.9	3.0
	C	3.6	3.3	3.6	3.5	3.5
+ 0.15	A	2.8	2.7	2.4	2.3	2.5
	B	3.7	3.1	3.3	2.9	3.3
	C	3.9	3.3	4.2	3.7	3.9
+ 0.20	A	3.3	3.3	2.3	2.4	2.6
	B	3.8	3.3	3.5	3.1	3.6
	C	4.0	3.6	4.3	3.7	4.6
+ 0.25	A	3.5	3.5	2.9	3.4	3.3
	B	3.9	3.6	3.7	3.6	4.1
	C	4.1	4.0	4.4	4.4	4.7
+ 0.30	A	3.3	3.4	2.8	3.7	3.0
	B	3.7	3.5	3.6	4.0	4.7
	C	4.0	3.9	4.4	4.5	4.8

Table 4. Relative r.m.s. intensity fluctuations in per cent in Hγ
A, B and C stand for the respective sizes

Δλ in Å		μ = 1.0	0.8	0.6	0.4	0.3
— 0.02	A	2.5	2.3	3.2	3.2	2.8
	B	2.7	3.0	2.8	3.0	2.6
	C	2.8	3.3	3.1	3.3	3.1
— 0.05	A	2.5	2.2	2.4	3.1	2.8
	B	2.7	2.8	2.8	3.6	3.1
	C	2.9	2.8	3.4	3.4	3.2
— 0.07	A	2.4	2.1	2.6	2.9	3.0
	B	2.9	3.0	2.9	2.9	3.1
	C	3.0	3.1	3.7	3.1	3.3
— 0.10	A	2.9	2.3	2.2	3.2	2.7
	B	3.1	2.9	2.7	3.0	3.3
	C	3.4	3.1	3.1	3.2	3.6
— 0.20	A	2.4	2.3	2.3	2.8	2.9
	B	2.5	2.6	2.7	3.5	3.5
	C	2.9	3.5	3.4	3.7	4.1
— 0.00	A	2.8	2.5	2.1	2.7	3.0
	B	2.9	2.0	2.7	2.8	3.0
	C	2.8	3.0	3.2	3.3	3.1
+ 0.02	A	2.4	2.5	2.2	2.7	2.9
	B	2.8	2.9	2.8	2.6	3.3
	C	2.9	3.0	2.8	3.1	3.5
+ 0.05	A	2.6	2.6	2.3	3.1	2.8
	B	3.2	2.9	3.1	2.9	3.6
	C	3.6	3.0	3.3	3.4	3.7
+ 0.07	A	2.1	2.5	2.1	3.7	2.7
	B	2.7	3.1	3.0	3.0	3.5
	C	2.9	3.2	3.2	3.5	3.5
+ 0.10	A	2.5	2.3	3.3	3.5	3.4
	B	2.8	3.0	3.3	3.2	3.4
	C	2.9	3.0	3.5	3.6	3.5
+ 0.20	A	1.9	1.9	2.7	3.1	3.3
	B	2.5	2.9	2.7	3.1	3.3
	C	2.8	3.2	3.0	3.6	3.3

Table 5. Relative r.m.s. intensity fluctuations in per cent in Hα
A, B and C stand for the respective sizes

Δλ in Å		μ = 1.0	0.8	0.6	0.4	0.3
— 0.05	A	2.3	2.1	2.7	2.9	3.7
	B	2.8	2.9	2.9	2.9	3.3
	C	3.1	3.1	3.3	3.2	2.6
— 0.10	A	2.1	2.0	2.4	2.9	2.6
	B	2.4	2.8	2.6	3.0	2.8
	C	3.2	3.0	3.1	3.4	2.7
— 0.15	A	2.4	1.9	2.2	2.7	2.6
	B	2.7	2.5	2.7	3.2	3.0
	C	3.1	2.9	3.2	3.4	2.7
— 0.20	A	2.3	2.0	1.7	2.7	2.5
	B	2.6	2.2	2.5	2.9	2.6
	C	3.1	3.0	3.1	3.4	2.7
— 0.25	A	2.4	1.7	2.5	2.5	2.4
	B	2.7	2.5	2.6	2.9	2.6
	C	3.1	3.0	3.0	3.3	2.8
— 0.30	A	2.2	1.8	2.1	2.3	2.1
	B	2.7	2.5	2.4	2.7	2.6
	C	3.1	3.0	3.2	3.0	2.8
0.00	A	2.6	2.4	2.5	3.2	3.5
	B	2.9	3.0	2.6	2.9	3.3
	C	3.4	3.3	3.1	3.4	3.1
+ 0.05	A	2.2	2.1	2.0	2.9	2.6
	B	2.7	2.7	2.5	2.7	2.9
	C	3.2	3.1	3.3	3.6	3.0
+ 0.10	A	2.2	1.8	1.7	3.0	2.2
	B	2.5	2.2	2.4	2.8	2.9
	C	3.2	3.0	3.3	3.8	2.8
+ 0.15	A	2.4	1.9	2.0	2.6	2.6
	B	2.6	2.7	2.7	2.9	2.9
	C	3.1	3.1	3.3	3.6	3.0
+ 0.20	A	2.5	1.9	2.1	2.2	2.3
	B	2.7	2.6	2.6	2.9	2.9
	C	3.0	3.1	3.1	3.5	2.8
+ 0.25	A	2.4	2.1	2.0	2.1	2.5
	B	2.7	2.6	2.6	2.8	2.7
	C	3.2	3.0	2.9	3.3	2.8
+ 0.20	A	2.4	2.0	2.0	2.1	2.4
	B	2.6	2.5	2.8	2.7	2.6
	C	3.2	3.0	2.8	3.0	2.9

Acknowledgement

We thank Mr. A. V. Raveendran for his help in the numerical computations.

References

Bappu, M.K.V., 1964, *J. Inst. Tele. Com. Eng.* 10, 388.
Behannon, K. W., Ness, N. F., *1966, NASA TND-3341.*
Bleckman, R. B., Tukey, J. W., 1958, *The Measurement of Power Spectra*, Dover Publications.
Canfield, R. C., Mehltretter, J. P., 1973, *Solar Phys.* 33, 33.
Cannon, C. J., Wilson, P. R., 1970, *Solar Phys.* 14, 29.
Cannon, C. J., Wilson, P. R., 1971, *Solar Phys.* 17, 288.
De Jager, C., 1957, *Bull astr. Inst. Netherl.* 13, 133.
Evans, J. W., Catalano, C. P., 1972, *Solar Phys.* 27, 299.
Evans, J. W., Michard, R., 1962, *Astrophys. J.* 136, 487.